Available online at www.sciencedirect.com
SCIENCE DIRECT
Vibrational Spectroscopy 39 (2005) 114–125
VIBRATIONAL SPECTROSCOPY
www.elsevier.com/locate/vibspec

Infrared and Raman spectroscopic study of pH-induced structural changes of L-histidine in aqueous environment

J. Gerbrand Mesu, Tom Visser, Fouad Soulimani, Bert M. Weckhuysen *

Utrecht University, Department of Inorganic Chemistry and Catalysis, Debije Institute, Sorbonnelaan 16, 3584CA Utrecht, The Netherlands

Received 29 November 2004; received in revised form 4 January 2005; accepted 6 January 2005
Available online 26 February 2005

Abstract

Aqueous solutions of L-histidine have been analysed in parallel by infrared (IR) and Raman spectroscopy over the pH range 0–14 with increments of one pH unit. The vibrational spectra in the region 2000–500 cm^{-1} have been interpreted and band positions have been assigned tentatively, taking into account assignments from literature after critical evaluation. As a result, a complete and complementary set of vibrational data has been obtained that can be used to determine all possible states of protonation of histidine, i.e. H_4His^{2+}, H_3His^{+}, H_2His^{0}, $HHis^{-}$ and His^{2-}. In addition, IR and Raman bands have been proposed as markers for the presence of the imidazole N^{π}- or N^{τ}-protonated tautomeric forms of H_2His^{0} and $HHis^{-}$.

Keywords: Amino acid; Tautomer marker; State of protonation; Vibrational assignment

1. Introduction

The elucidation of the secondary and tertiary structures of amino acid side chains has been subject of research for many years. This is largely due to the fact that the spatial orientation plays a key role in the folding/unfolding ability of peptides and in the catalytic activity of enzymes. The pH is one of the driving forces in the orientation process, as it affects the state of protonation and hence the formation of hydrogen bridges and the number of binding sites for ions of transition metals such as Cu, Fe and Co. An amino acid of major importance as a ligand in many metallo-enzymatic reactions is histidine [1]. Due to the presence of an imidazole ring, the molecule possesses three extra potential sites for (de)protonation and metal binding in addition to the two (NH_2 and COOH) amino acid end groups. Besides, for two of the ionic structures, histidine can be present in two pH-dependent tautomeric forms. As a consequence and as result of its flexible structure, histidine can occur in several pH-dependent states of protonation and coordination, either as part of a peptide backbone or as a free ligand molecule.

Next to NMR, infrared (IR) and Raman spectroscopy are commonly applied to obtain this type of structural information, as both techniques can be applied in vivo and over a wide pH range. Besides, the short time scale of vibrational absorption and relaxation in relation to the lifetime of free rotating structures and tautomeric equilibriums, allows simultaneous qualitative and quantitative observation of all structures and ionic forms that are present in a chemical or biological system. Finally, IR and Raman are complementary techniques, which implies that an almost complete vibrational analysis is possible, particularly when combined with theoretical calculations. As a result, many vibrational spectroscopic studies on histidine and related imidazole-type compounds have been carried out, providing a considerable amount of data in the literature, occasionally summarized in reviews [2–8] and books [9,10]. To our knowledge, normal coordinate analysis (NCA) on histidine has not been carried out thus far and the first ab initio and density functional theory (DFT) study on the molecule was published only very recently [11]. However, this research concerned the conformational dependence of the pK_a values

* Corresponding author. Tel.: +31 302537400; fax: +31 302511027.
E-mail address: b.m.weckhuysen@chem.uu.nl (B.M. Weckhuysen).

0924-2031/$ – see front matter © 2005 Elsevier B.V. All rights reserved.
doi:10.1016/j.vibspec.2005.01.003

and not a vibrational analysis. For that reason, only results of theoretical calculations on the model compounds imidazole [12,13], 4-methyl-imidazole [12,14–17] and 4-ethyl-imidazole [18] have been used to support the conclusions from empirical IR and Raman studies of histidine [19–36] and closely related molecules [37–41]. The majority of this research has been focussed on IR or Raman bands that can be used as a marker to determine the state of protonation of the imidazole nitrogen atoms [15,16,20–27] or the type of metal ion binding [24,29,32,34,37,39,40] and thus, measurements have been performed mainly at physiological conditions or at specific pH values close to the pK_a values of the different active sites. Besides, samples have often been measured in D_2O or after crystallization to circumvent interference from water bands. As a consequence, there are large gaps in the availability of experimental vibrational data and assignments in H_2O, while an integrated IR and Raman study on aqueous solutions of histidine has to, our knowledge, not been published so far. Moreover, we noticed that some of the assignments and conclusions in literature are inconsistent or even conflicting. In order to clarify these controversies and obtain the lacking vibrational data, we decided to carry out systematic and detailed IR and Raman measurements of histidine at well-defined experimental conditions. However, the main motivation for this work is to extend the pH region to high and low values, as this is important in the field of the functionalization of inorganic substrates such as zeolites, with amino acid complexes [42,43]. These combined organic/inorganic materials are expected to have high potentials, not only in biomedical applications, but also as sensors, catalysts and molecular electronic devices [44]. For a better understanding and optimization of the structure/activity relationship, it is important to have insight into the precise molecular structure and structural behaviour of the amino acids at pH values beyond that in biological systems. For that reason, aqueous solutions have been measured in parallel with both techniques in the spectral region 2000–500 cm^{-1} from pH 0 to 14 with increments of one pH unit. The resulting set of complementary spectral data has been interpreted and tentatively assigned to vibrational modes. In addition, the spectral data have been translated to bands that can be used as markers for the state of protonation, taking into account data and assignments from literature after careful comparison and evaluation. As a result, a more complete picture of histidine emerges.

2. Materials and methods

2.1. Chemicals and solutions

L-Histidine (p.a. grade) was obtained from Acros Organics (Geel, Belgium). Solutions were freshly made by dissolving solid L-histidine in distilled water at a concentration of 38 g/L. Dissolving was promoted by exposure of the fresh made solution to an ultrasonic bath during 20 min. Solutions were made acidic by addition of HCl and basic by addition of NaOH. The pH was determined at ambient temperature (21 °C) with a pH meter model PHM 210 from Radiometer Analytical (USA). In order to check the conversion reversibility from one state of protonation to another, titration experiments from pH 0 to 14 and backwards have been carried out. The resulting IR and Raman data revealed full reversibility, which proves that degradation did not occur.

2.2. Infrared spectroscopy

IR measurements were carried out at room temperature on a Perkin-Elmer 2000 Fourier transform spectrometer equipped with a DTGS detector. The sample compartment was flushed with dry air to reduce interference of H_2O and CO_2. Spectra were recorded with a horizontal ATR accessory (Spectra-Tech) equipped with a ZnSe crystal as the reflecting element. Data point resolution of the spectra was 4 cm^{-1} and 100 scans were accumulated for one spectrum. Spectral interpretation was carried out after subtraction of the spectrum of water at the corresponding pH as background.

2.3. Raman spectroscopy

Raman measurements were carried out on a Kaiser RXN spectrometer equipped with a 70 mW 785 nm diode laser for excitation, a holographic grating for dispersion and a Peltier-cooled Andor CCD camera for detection. Spectra were recorded in glass vials (Spectra-Tech) at room temperature. Detector pixel resolution was about 2 cm^{-1} and 15 scans were accumulated for one spectrum at an exposure time of 30 s per scan. Subtraction of the water background has not been applied for the Raman spectra.

3. Results and discussion

According to literature [16,23–25,31,32,45,46] histidine can be present in five different pH-dependent ionic forms, which are shown in Fig. 1. In addition, the pK_a values of the different sites of protonation have been indicated according to [24]. Furthermore, as has been depicted, the ionic structures H_2His^0 and $HHis^-$ can occur in two different tautomeric forms, since the nitrogen atoms of the imidazole ring are not identical. The commonly accepted notation to distinguish for (de)protonation of both atoms is N^{π} for the nitrogen atom which is closest to the CH_2 group and N^{τ} for the other one. Additionally, Blomberg et al. [46] proposed a third tautomeric form for H_2His^0 with an intramolecular H···N bonding as indicated in Fig. 1. Theoretically, it should be possible to distinguish all these structures by differences in their vibrational spectroscopic features. Obviously, assignment will be relatively easy for bands related to characteristic functional group modes and

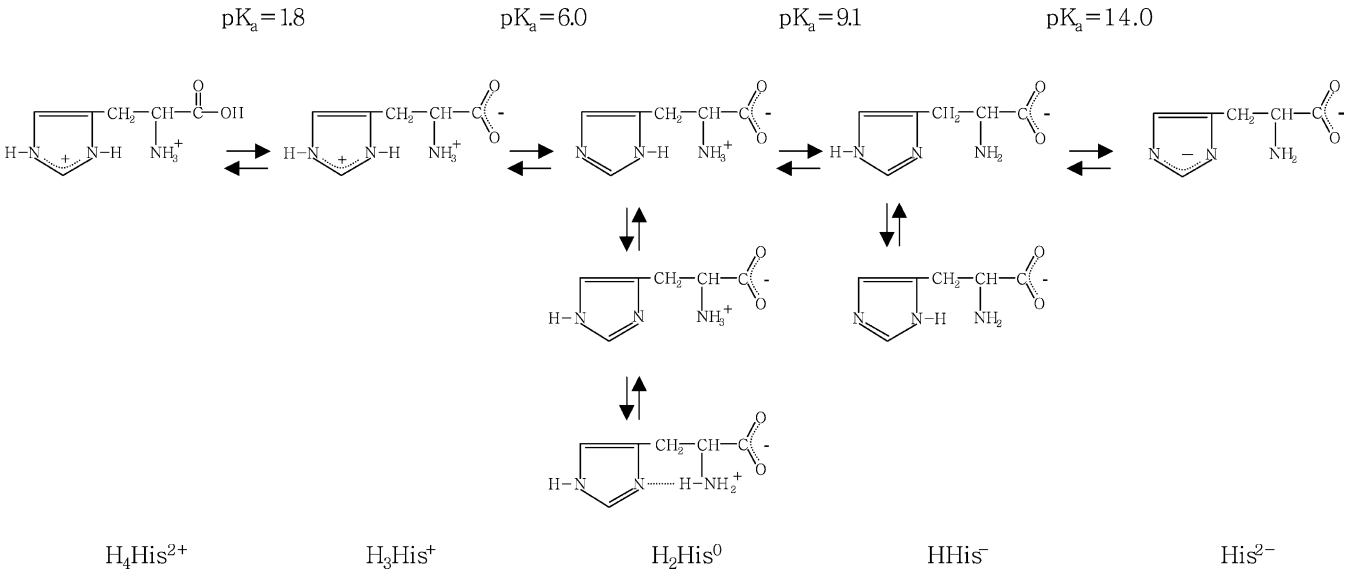

Fig. 1. Proposed structures of the different states of protonation and tautomers of L-histidine in aqueous solution. The pK_a values have been taken from [24].

provided the vibrations are sufficiently affected by a change in conformation or tautomeric form to be visible in the spectra. In contrast, less sensitive vibrations and less dramatic structural differences, such as between the three tautomeric forms of H_2His^0, will be more difficult to distinguish with IR and Raman, particularly since a change in the dielectric constant of the solution as result of changing the pH or buffer concentration may cause frequency shifts as well. Hence, well-controlled experimental conditions have been applied to obtain accurate spectral data. For that reason, the same aqueous solutions of L-histidine have been measured in parallel by IR and Raman spectroscopy over the full pH range of 0–14. Besides, pH increments of one have been applied for the solutions in order to monitor even small pH effects on the spectra. A selection of the IR and Raman spectra is presented in Figs. 2 and 3, respectively. For reasons of clarity, only spectra at even pH values are displayed. The observed IR and Raman band positions of all spectra including the estimated positions of shoulders are summarized in Tables 1 and 2, respectively. Assignments for most of the observed bands are proposed after spectral interpretation, taking into account IR and Raman selection rules and assignments extracted from literature. Data and assignments from literature have been carefully evaluated and occasionally simplified to obtain a fair compromise between the results from different theoretical models and from various experimental conditions (e.g. solutions in H_2O or D_2O, powders and single crystals, HCl salts, etc.).

3.1. IR and Raman band assignments

3.1.1. The amino acid end group

In a highly acidic environment, histidine will be present mainly in the ionic form H_4His^{2+} (Fig. 1) with all nitrogen atoms and the carboxylic acid group protonated. Indeed, the strong C=O stretching band at 1736 cm^{-1} in the IR spectrum at pH 0 (Fig. 2) and the much weaker one in Raman (Fig. 3), confirm the protonated state of the carboxyl group. The same can be concluded from the strong IR band at 1257 cm^{-1},

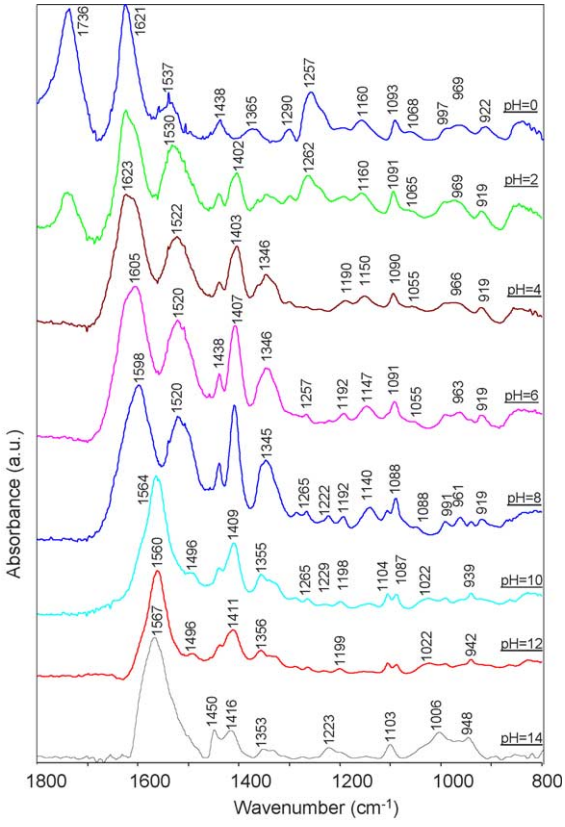

Fig. 2. Infrared spectra of aqueous solutions of L-histidine at pH 0, 2, 4, 6, 8, 10, 12 and 14.

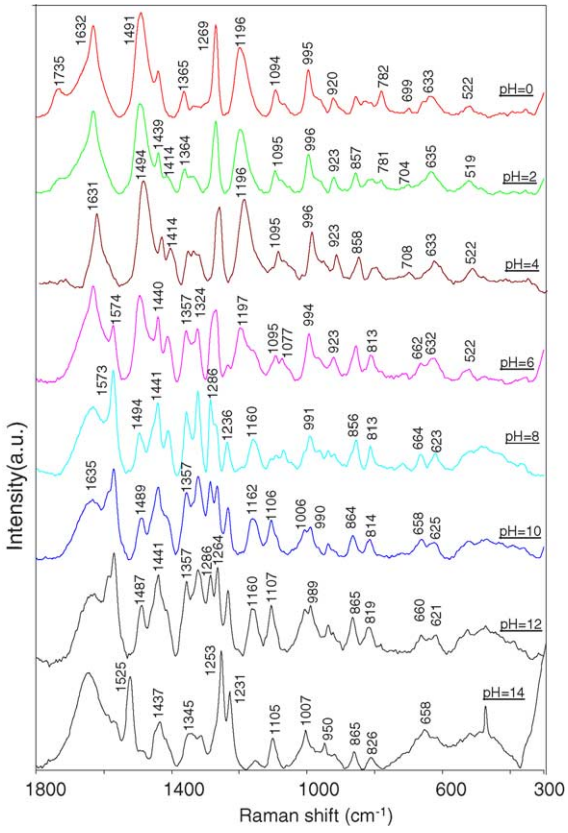

Fig. 3. Raman spectra of aqueous solutions of L-histidine at pH 0, 2, 4, 6, 8, 10, 12 and 14.

which can be assigned to νC–O in accordance with literature [23,24,26]. In line with the pK_a of 1.8 of the carboxyl group, the relative intensity of both bands decreases at pH 1 and the bands disappear at pH >2, illustrating deprotonation to CO_2^- and conversion to H_3His^+.

Simultaneously with the decreasing intensity of νC=O and νC–O in the IR spectra, the appearance of the anti-symmetric and symmetric C–O stretching vibrations of the CO_2^- group around 1620 and 1410 cm^{-1}, respectively, also marks the conversion from H_4His^{2+} to H_3His^+. Referring to the general literature [9,10], both modes should show medium to high IR, but low Raman activity and indeed, as can be seen from Fig. 2, a band arises in the IR spectrum around 1402 cm^{-1} at pH 2, which can be assigned straightforward to $\nu_sCO_2^-$ [9,10,23,26,27]. The vibration remains visible in IR and slowly increases up to 1416 cm^{-1} at pH 14. Assignment of the IR band at 1620 cm^{-1} to $\nu_{as}CO_2^-$ seems obvious, but contrary to some reports [23,24,27,40], the peak cannot be attributed to $\nu_{as}CO_2^-$ solely, since a band at this position is also observed in the IR spectrum of the fully protonated form H_4His^{2+} at pH 0. A plausible explanation is, that $\nu_{as}CO_2^-$ coincides with $\delta_{as}NH_3^+$, a vibration which is also expected to exhibit strong IR, but weak Raman activity around 1620 cm^{-1}. Comparison of the IR spectrum at pH 0 with those recorded at higher pH values reveals the appearance at pH 2 of a shoulder at the low frequency side of the 1620 cm^{-1} band that further increases in intensity with the pH. For that reason, we assign the initial band maximum at 1620 cm^{-1} band to $\delta_{as}NH_3^+$ and the low frequency shoulder at 1600 cm^{-1} to $\nu_{as}CO_2^-$. The correctness of this assignment is further evidenced by the increasing intensity of the latter at higher pH. At pH $\geq$6, $\nu_{as}CO_2^-$ becomes even more intense than $\delta_{as}NH_3^+$, which results in a red shift of the band maximum to 1600 cm^{-1}. In accordance with the pK_a value of 9.1, the NH_3^+ group becomes deprotonated at pH >9 and consequently, a contribution of $\delta_{as}NH_3^+$ is no longer visible in IR. The conversion from H_2His^0 to $HHis^-$ is also marked by a considerable drop of $\nu_{as}CO_2^-$ from 1600 to 1560 cm^{-1} and as expected, this IR band remains present up to pH 14 together with $\nu_sCO_2^-$ around 1410 cm^{-1}.

Next to the anti-symmetric bending vibration of the NH_3^+ group around 1620 cm^{-1}, the protonated state of the primary amino group seems also to be correlated to the medium to strong IR band around 1530 cm^{-1} (Fig. 2). Some papers report a band at this position to be mainly a C=C/C=N ring stretching vibration [14,28], but in acidic and neutral environment, we believe the largest contribution to the observed band originates from $\delta_sNH_3^+$ for the following reasons. Alike $\delta_{as}NH_3^+$, the frequency of the vibration shifts downwards on increasing pH and disappears in accordance with the pK_a at pH >9. The absence of a Raman counterpart and the large bandwidth, probably as result of hydrogen bonding interactions, are two other arguments. Finally, the correlation between $\delta_sNH_3^+$ and the presence of an IR band at 1530 cm^{-1} has been illustrated in literature by the disappearance of the band upon deuteration of the NH_3^+ group using glycine [48] and histamine [49] as model compounds.

It should be noted, that one might expect the appearance of the NH_2 scissoring vibration around 1600 cm^{-1} in the IR spectrum at pH >9 simultaneously with the disappearance of the NH_3^+ related bands. Indeed, closer examination of the $\nu_{as}CO_2^-$ band at 1560 cm^{-1} on pH 10–13 reveals some asymmetry at the high frequency side, but apparently the contribution is too weak to be observed as a separate band.

3.1.2. The side chain CH_2 and CH groups

The band around 1440 cm^{-1} in both IR and Raman can be easily assigned to the CH_2 scissoring vibration [23,26,28,50,51]. Since this alkyl group is neither subject to protonation nor very sensitive to solvent pH effects, its vibrational frequency and intensity are almost unaffected throughout the pH range 0–14. According to literature, CH_2 deformation vibrations also contribute to the complex IR bands between 1365 and 1325 cm^{-1} [23,27,28,47,50,51]. We partly agree on this assignment for the spectra recorded at low and high pH, but in view of the considerably increased intensity and broadening of the 1346 cm^{-1} component at pH 6–9, we also assume a substantial

Table 1
Observed infrared absorption frequencies of aqueous solution of histidine in the pH range 0–14

pH 0	pH 1	pH 2	pH 3	pH 4	pH 5	pH 6	pH 7	pH 8	pH 9	pH 10	pH 11	pH 12	pH 13	pH 14	Assignment	References
1736	1737	1738													νC=O	[9,10,23,24,26]
1621	1624	1623	1623	1623	1622	1623(s)	1620(s)	1620(s)							$\delta_{as}NH_3^+$	[9,10,26]
		1606(s)	1610(s)	1611(s)	1609(s)	1605	1599	1598	1593	1594(s)					$\nu_{as}CO_2^-$	[9,10,27,28]
									1570	1564	1560	1560	1564	1567	$\nu_{as}CO_2^-$	[9,10,27,28]
1537	1535	1530	1522	1522	1521	1520	1520	1520	1517						ν Ring/$\delta_s NH_3^+$	[13,23,28]
							1498(s)	1496(s)	1496(s)	1496	1496	1492			δN–H i.p./νC=N	[15,16,18,21]
1438	1440	1438	1438	1438	1438	1438	1438	1439	1438	1438	1437	1437	1440	1450	δCH_2	[23,26,28,50,51]
	1402	1404	1403	1403	1404	1407	1408	1408	1408	1409	1410	1411	1415	1416	$\nu_s CO_2^-$	[9,10,23,26,27]
1365	1363(s)	1361(s)	1361(s)	1361(s)	1361(s)	1362(s)	1355(s)	1356(s)	1354	1355	1355	1356	1355	1353	δCH_2 wagging	[23,27,28,40,50,51]
			1346	1346	1346	1346	1346	1346	1346						βNH_3^+	–
			1340(s)	1340(s)	1340(s)	1340	1336(s)	1335(s)	1340	1339	1337	1335(s)	1333	1332	βCH_2	[23,40,51]
			1328(s)	1328(s)	1329(s)	1326(s)	1324(s)	1321(s)	1322(s)	1328(s)	1326(s)		1326(s)		δCH_2/δ=C–H	[23,27,28,47]
1295(s)	1297	1297	1299	1300	1299										νC=N + δ=C–H	[12,14,28,50]
							1284	1284	1287	1286	1284	1287	1280	1275	ν=C–N + δC–H	[6,12,14–18]
			1265	1265	1264	1267	1265	1265	1265	1263	1262	1262			ν=C–N + δC–H	[6,12,14–18,34]
1257	1260	1262													ν_sC–O	[9,10,23,24]
1240(s)	1238(s)	1238(s)	1239	1239	1239	1221	1222	1222	1223	1229	1229	1230	1230	1223	νC–N + C–C + δC–H	[6,12,14,15,17,18]
1190(s)	1190(s)	1192	1190	1187	1191	1192	1192	1192	1193	1198	1199	1199	1198	1198(s)	δ–C–H (γCH_2)	–
1161	1160	1155	1152	1151	1149	1147	1142	1139	1141	1144	1147	1152	1151	1149	ν=C–N/δ=N–H	[13–17,26]
						1106(s)	1106	1104	1104	1104	1104	1104	1104	1103	ν=C–N/δ=C–H(N^{π})	[14–17,23,25–26]
1094	1094	1094	1093	1093	1093	1091	1089	1088	1088	1087	1087	1087	1088		ν=C–N/δ=C–H(N^{τ})	[14–17,23,25–27]
1068(s)	1066(s)	1065(s)	1055	1055	1054	1055(s)	1049	1048	1046	1022	1024	1022	1022(s)	1006	νC–N side chain	–
997	991	991	990(s)	993(s)	990(s)	990	990	991	991	990	991	990	991		ν=C–N/δ ring	[16,25]
969	970	969	969	966	965	963	961	961	961	960(s)					δ NH_3^+	–
						940(s)	940	939	940	939	939	940	942	948	δ Ring	[12,15–18,27,29]
922	920	919	919	919	919	919	919	919	919	922(s)					δ=C–H i.p.	[12,30,51]
856	851	855	855	855	855	850									δ Ring i.p./NH_3^+ rock	[23,27,28,37]

Coupled vibrations are indicated by "+" and coinciding modes by "/". Wavenumbers with indication (s) are shoulders.

Table 2
Observed Raman shifts of aqueous solutions of histidine in the pH range 0–14

pH 0	pH 1	pH 2	pH 3	pH 4	pH 5	pH 6	pH 7	pH 8	pH 9	pH 10	pH 11	pH 12	pH 13	pH 14	Assignment	References
1735	1735	1735													νC=O	[9,10,23,24,26]
1632	1632	1632	1631	1631	1631	1632									νC=C + νC=N	[21,22,31,32,35]
										1588	1587	1589	1588	1524	νC=C + νC=N(N^{π})	[15,16,18,31]
					1574(s)	1574	1573	1573	1573	1572	1572	1571	1572		νC=C + δN–H(N^{τ})	[15,16,18,31]
1491	1492	1492	1494	1494	1492	1496	1494	1494	1494	1489	1489	1487	1492		δN-H i.p.	[15,16,18,21]
1439	1439	1440	1439	1440	1439	1440	1441	1441	1441	1441	1440	1441	1440	1451	δCH_2	[23,28,50,51]
		1414	1413	1412	1414	1412	1412	1411	1412	1417(s)	1415(s)	1416(s)	1423	1423	δCH–(CO_2^-)	–
1365	1362	1364	1363	1363	1363										δCH_2/ν ring	[16,24,34]
						1357	1356	1355	1356	1357	1356	1358	1357	1345	νC=N + νC–C(N^{π})	[16,23,28,34]
			1346	1346	1347(s)										ν Ring (C–N)	[16]
1330	1332(s)	1335	1335	1338(s)	1340										ν Ring (C–N)	[16]
1325	1328	1329(s)	1328(s)	1328(s)	1327(s)									1317	δCH_2	[16,18,34,50]
						1324	1323	1322	1323	1322	1323	1321	1322		νC=N + νC–N(N^{τ})	[16,23,24,34]
			1276(s)	1277(s)	1276(s)	1281(s)	1285	1286	1286	1286	1286	1287	1286		ν=C-N + νC–C(N^{τ})	[16,21]
1269	1269	1270	1269	1269	1269	1269	1268	1268(s)	1267	1264	1264	1264	1264		δ=C–H(N^{π})	[16,21,34]
														1253	δ=C–H	[34]
						1236	1235	1235	1234	1233	1234	1233	1235	1230	δ=C–H + ν=C–N	[14,16]
1197(s)	1198	1198	1199	1196	1196	1197									νN–C–N + δN–H i.p.	[14,21,22]
						1164(s)	1160	1158	1160	1162	1160	1160	1154	1155	ν=C–N + δN–H	[12–17]
							1106(s)	1107	1105	1105	1106	1105	1107	1105	ν=C–N + δ=C–H(N^{π})	[14–17,23,25,27]
1094	1094	1095	1095	1095	1095	1096	1089	1090	1091	1094(s)	1090(s)				ν=C–N + δ=C–H(N^{τ})	[14–17,23,25,27]
1078(s)	1079(s)	1074(s)	1075(s)	1074	1077	1072	1070	1070(s)							δ=N–H i.p. (N^{τ})	[21,22]
							1007(s)	1009(s)	1009	1006	1008	1006	1008	1007	δ=C–H i.p. (N^{τ})	[16,21,22]
995	996	996	997	996	996	994	991	991	991	990	989	989	990		ν=C–N + δ ring (N^{π})	[16,21,22,37]
975	972	970(s)	970(s)	968(s)	970(s)	970(s)	967	963	966	970(s)					ν=C–N + δ ring	[14–17,37]
						936	937	938	937	937	937	937	938	950	δ Ring i.p.	[12,15–18,27,29]
922	922	923	922	923	922	923	922	920	921	922	923(s)	925			=C–H i.p.	[12,30,51]
855	857	855	856	858	857	856	855	856	856	864	865	865	863	865	ν=C–C + δ ring	[16,23,24,27]
824	824	818(s)	818(s)	820(s)	816(s)										δ=C–H o.o.p.	[14,15,17,18,50]
810	810	810	808	812	808	813	813	813	814	814	817	819	821	819	δ=C–H o.o.p.	[14,15,17,18,50]
782	781	782													δCOOH	
699	700	704	706	708	708	710	710(s)	718	718						δ Ring	[21,24,34]
655	655	661(s)	660(s)	656(s)	650(s)	662	663	664	662	666(s)	662	660	662	657	δ Ring	[14–17,21,23,50]
632	637	635	634	633	633	632	623	622	622	622	623	621			δ Ring	[14–17,21,23,50]
522	519	519	519	522	518	522	524	523	525	524	522	524			?	

Coupled vibrations are indicated by "+"and coinciding modes by "/". Wavenumbers with indication (s) are shoulders.

contribution of another vibration that is related to the ionic state H_2His^0. The large bandwidth points to a mode in which hydrogen bonding is involved, e.g. a NH_3^+ wagging or a vibration that is related to the intramolecular bridged tautomer of H_2His^0 as depicted in Fig. 1, but we have no further proof for this hypothesis. Furthermore, a ring =C–H deformation might as well contribute to the weak band around 1325 cm^{-1} [23,27,28]. Vice versa, a contribution of the CH_2 wagging vibration to the Raman bands in the same region cannot be excluded [18,24,34,47,50], but as pointed out later, we believe that the largest intensity originates from skeletal modes.

3.1.3. Imidazole C=C and C=N vibrations

At low pH, a sharp intense peak at 1632 cm^{-1} is superimposed on the weak O–H deformation band of water in the Raman spectra. The peak starts to disappear at the pK_a value of the protonated imidazole group, i.e. at pH 6 (see Fig. 3) and it is therefore a good marker for the conversion of H_3His^+ to the zwitterionic state H_2His^0. Simultaneously, a peak at 1574 cm^{-1} shows up and remains present up till pH 13. Since both bands are strong in Raman, but virtually absent in IR, it seems obvious to assign the band at 1632 cm^{-1} to predominantly the C=C stretching vibration of the protonated imidazole ring (conformers H_4His^{2+} and H_3His^+) and the band at 1574 cm^{-1} to the weakened νC=C of the neutral and negatively charged ring (conformers H_2His^0, $HHis^-$ and His^{2-}). In view of the relatively large sensitivity of the band to protonation, some coupling with C=N stretching will probably occur. The same holds for a second Raman band, that appears at 1588 cm^{-1} at pH >9 and remains present up till pH 13. The simultaneous presence of two C=C bands can be explained only by assuming the presence of two tautomeric forms of $HHis^-$ as indicated in Fig. 1, i.e. with either N^π- or N^τ-protonated. Indeed, as empirically demonstrated by Ashikawa and Itoh [21,22] and confirmed by others [16,18,31], the 1588 cm^{-1} band appears to be correlated to the N^π-protonated tautomer and the 1571 cm^{-1} one to the N^τ-protonated form. From the strong intensity of the latter compared to that of the 1588 cm^{-1} peak it can be concluded, that protonation of N^τ is preferred over protonation of N^π, which is in line with the results of a temperature dependency studies of histidine by means of NMR [45] and of 4-methyl-imidazole by Raman [16]. The fact that the 1588 cm^{-1} component is even virtually absent below pH 9 can be interpreted as absence (or largely reduced presence) of the N^π-protonated form of H_2His^0. Furthermore, it can be concluded that the sensitivity of the C=C vibrational frequency for (de)protonation of N^π or N^τ points to either an inductive effect of N-protonation or to coupling of the C=C vibration with =C–N, =C–C or =C–N–H modes. According to DFT calculations on 4-methyl-imidazole and 4-ethyl-imidazole [15,16,18] coupling of δN–H and νC=C indeed occurs, but only in the N^τ-protonated tautomer. This explains the difference in band position compared to the N^π-protonated form. Obviously, complete deprotonation of the imidazole ring (pK_a = 14) will affect the C=C vibration and as can be seen from Fig. 3, the C=C region in the Raman spectra changes dramatically at pH >13, which marks the conversion from $HHis^-$ to His^{2-}. The C=C bands around 1570/1580 cm^{-1} disappear completely and a new strong band shows up at 1525 cm^{-1}. The drop in the vibrational frequency can be explained by a further decrease of the bond C=C strength, while the increased symmetry of the imidizole ring explains the strong Raman activity. It should be noted, that the imidazole C=C vibration might exhibit some minor IR activity as well, but a contribution to the IR bands of $\nu_{as}CO_2^-$ and $\delta_{as}NH_3^+$ in the region 1620–1570 cm^{-1} is not observed.

Assignment of a band to the C=N stretching mode is more difficult due to the unlocalized character of this vibration, i.e. coupling to νC=C, and the possible resonance structures of the imidazole ring in the ionic structures H_4His^{2+}, H_3His^+ and His^{2-}. According to literature, the corresponding band around 1600 cm^{-1} should be medium in Raman and weak in IR, but no peak is found at this position that points towards the conversion of H_3His^+ to H_2His^0 or from $HHis^-$ to His^{2-}.

3.1.4. Imidazole skeletal modes

The dominating peak in the Raman spectra at low pH is found at 1491 cm^{-1}, but there is no consensus on the assignment in literature. The band has been reported as an N–H in-plane bending [21] and as a ring stretching combined with =C–H bending [23,29] for histidine, and to a coupled ring δN–H/νC=N mode for 4-methyl-imidazole and 4-ethyl-imidazole [15,16,18]. Coupling of vibrations undoubtedly plays a role, and in agreement with [15,16,18,21] we believe the band to be predominantly an in-plane N–H bending/C=N stretching vibration for two reasons. Firstly, the band disappears upon deuteration, as shown by Toyoma et al. [16], which implies that the ring nitrogens are largely involved. Secondly, the largest Raman activity of the vibrations can be expected for the positively charged imidazole ring (H_4His^{2+} and H_3His^+), as the ring is highly symmetrical due to protonation of both N^π and N^τ. The fact that the Raman intensity drops at pH >6 upon partial deprotonation of the ring and completely disappears at pH 14, where both N^π and N^τ are deprotonated, is in line with this assignment. The same holds for the weak IR activity as a band at the same position is only observed at pH 8–12.

Assignment of the Raman band at 1414 cm^{-1} to a coupled ring N–H bending/C–N stretching mode as indicated by the results of DFT calculations on 4-methyl-imidazole and 4-ethyl-imidazole [15,18], is rejected as the band is still present when the ring is completely deprotonated, i.e. at pH 14. Attribution to $\nu_sCO_2^-$, as proposed in literature [24,34,35], is also neglected since the Raman shift is significantly higher than the position of this vibration in IR. On the other hand, the band arises at pH 2 and remains present up to pH 14 and hence, a correlation to the deprotonated carboxyl group seems more obvious than to

an imidazole ring vibration. For that reason, we tentatively assign this band to a CO_2^- related mode without further detail on the type of vibration.

Several other bands, which are prominent in Raman but weak in IR, can be attributed to imidazole skeletal modes. In accordance with the results of normal coordinate analysis of 4-methyl-imidazole [16], we assign the intense pair of Raman bands around 1357 and 1324 cm^{-1} in the pH range 6–13 to coupled C=N and =N–C ring stretching vibrations, the high frequency one being characteristic for N^{π} protonation and the low frequency band for the N^{τ}–H form of the ionic states $HisH^0$ and His^-. However, at lower pH (0–5), a Raman band is present at 1365 cm^{-1}, which must be due to another vibration in view of its shifted position and significant lower intensity. We reject the assignment of Garfinkel and Edsall [19] of a $\nu_s CO_2^-$ because of the absence of a strong band in IR, but in line with the IR data, a CH_2 wagging is a plausible explanation. On the other hand, we believe that a ring-stretching mode of the protonated imidazole ring [16,34] contributes to the observed band as the presence of the peak appears to be correlated to H_4His^{2+} and H_3His^+. A similar explanation can be given for the Raman band at 1325 cm^{-1}. As pointed out earlier, this peak is intense at pH 6–13 but a weak band at the same position is also observed at other pH values as well as in the IR spectra. For that reason we also propose a contribution of a CH_2 deformation vibration next to the previously mentioned coupled C=N/=N–C mode [16,34]. The weak Raman shifts between 1330 and 1347 cm^{-1} have not been referred to in literature. Band maxima are only clearly visible in the spectra of pH 0–5 and for these bands we propose a stretching vibration of the enhanced ring C–N bond strength in the ionic states H_4His^{2+} and H_3His^+ [16].

It is generally agreed that the IR and Raman bands below 1300 cm^{-1} originate from coupled skeletal stretching and bending modes of C–N, C–C, N–H and C–H which are, therefore, not well localized. On the other hand, it is obvious to assign the strong Raman band at 1269 cm^{-1} in acidic environment (pH <6) to an imidazole ring breathing vibration [21,22], regarding the high symmetry of the ring in the ionic forms H_4His^{2+} and H_3His^+. However, at pH >3, a second band around 1285 cm^{-1} grows in and both bands have been assigned to mainly a ring type of =C–H in-plane bending by Stewart and Fredericks [34]. This is in line with the results of normal coordinate analysis of 4-methyl-imidazole [14,16] for the 1265 cm^{-1} peak but, on the contrary, the 1285 cm^{-1} band has been calculated as a coupled C–C=/=C–N stretching vibration. The fact that both vibrations show only minor IR activity does not contradict to these assignments. It should be noted, however, that the empirical correlation of the 1285 cm^{-1} band to the N^{τ}-protonated and the 1265 cm^{-1} one to the N^{π}-protonated tautomeric form of H_2His^0 and $HHis^-$ as reported in the literature [16,21] is only valid for the pH range 9–13. As a shoulder at 1285 cm^{-1} is already present at pH 3, it implies that the bands are only useful as a marker for the conversion from one ionic state to another when the intensity is taken into account.

The Raman band at 1236 cm^{-1} that appears at pH >6 has been assigned to a coupling of ν_sN–C–N and an in-plane N–H bending by Ashikawa and Itoh [21,22], while Majoube et al. [14] suggested a ring =C–H bending for 4-methyl-imidazole. The latter is partly in accordance with Toyoma et al. [16] who calculated the band to be an overlap of a =C–N stretching of the N^{π}–H tautomer and a =C–H bending of the N^{τ}–H counterpart. We follow this assignment up till pH 13. However, our data show that a band at 1230 cm^{-1} is also present at pH 14, where the imidazole ring is unprotonated, which excludes more or less a nitrogen involved ring vibration at least for the ionic state His^{2-}. For that reason, we believe this band to originate from an in-plane =C–H bending in accordance with [14]. The absence of a significant IR band is in line with this proposal. Literature assignments of the very weak IR bands that we observe in the same region are absent, probably due to the lack of intensity, but as the IR bands around 1284 and 1265 cm^{-1} largely overlap with the positions found in Raman it seems obvious to follow the same assignment. Indeed, it probably concerns coupled =C–N stretching modes [15–18], and/or =C–H deformation modes [6,12,14], but in view of the weak intensities, the usefulness as tautomer markers is poor.

The intense Raman band around 1196 cm^{-1} at pH 0 disappears at pH >6 which makes it a good marker for $H_4His_2^+$ and H_3His^+. The high intensity points to a symmetrical mode of the double protonated imidazole ring, either a type of ring breathing or a combination of ν_sN–C–N with an in-plane N–H bending [14,21,22]. A band around 1196 cm^{-1} is also observed in IR, but the intensity is low and the band is present throughout the pH range 0 to 14. Only one reference has been found in literature for an IR band at this position, i.e. at pH 7.7, and it has been assigned to a in-plane ring deformation [26]. Contrary to what the authors report, we observe hardly any effect of the pH and for that reason we assume it is a pH insensitive vibration side chain –C–H deformation, possibly a rocking CH_2 vibration. The weak IR band in the region 1160–1140 cm^{-1} has also not been mentioned in papers on histidine and therefore we follow the assignment based on theoretical calculations on imidazole [13] and 4-methyl-imidazole [14–17]. Accordingly, we assign the band to a coupled ν=C–N/δ=N–H vibration of which the calculated potential energy distribution points to predominantly =C–N stretching. A band also shows up around 1160 cm^{-1} in the Raman spectra at pH 6 which largely weakens at pH 14. In view of this property, it can be regarded as a good marker for the ionic states H_2His^0 and $HHis^-$. At some pH values, the difference between the IR and Raman band maxima is significantly larger than the instrumental resolution, which implies that it concerns principally two different modes. Yet, in line with the theoretical calculations, we assign the band to similar types of (coupled) ring =C–N stretching and/or =N–H bending vibrations.

The IR and Raman bands around 1106 and 1090 cm^{-1} exhibit more or less the same behaviour in the sense that the former arises concomitantly in the IR and the Raman spectra at pH >6, while the contribution at 1090 cm^{-1} is present from pH 0 up to 13, in Raman as a shoulder and in IR as a separate band. Different from empirical correlations [21], ab initio DFT calculations and normal coordinate analysis on 4-methyl-imidazole [15–17] indicate that the bands are mainly ring =C–N stretching vibrations coupled to the corresponding =C–H in-plane deformation. This is in accordance with the assignments proposed by others [14,23,25–27]. Obviously, the intensity in IR and Raman differ due to different activity, but the fact that two peaks are present in the pH range of H_2His^0 and $HHis^-$ (pH 6–13) can be explained by the sensitivity of the imidazole nitrogen atoms to protonation. Hence, the small bands are useful as tautomer markers, particularly in IR, the 1105 cm^{-1} component representing the N^{π}-protonated form and the 1090 cm^{-1} one the N^{τ}–H form [15,17,25].

Assignments of the weak IR and Raman signals between 1070 and 1020 cm^{-1} have not been found in the literature for histidine and imidazole type of compounds. In contrast, for amino acids a band in this region is usually assigned to a C–N stretching vibration [9,10]. The position of the IR band suggests a correlation to the ionic form of histidine, as the downward 'jumps' in frequency from 1068 cm^{-1} (pH 0) to 1055 cm^{-1} (pH >2), 1048 cm^{-1} (pH >6), 1022 cm^{-1} (pH >9) and 1006 cm^{-1} (pH 14) corresponds surprisingly well to the different pK_a values. In view of the central position of the carbon atom attached to the primary amino group with respect to the different sites that can be protonated, we propose a side chain C–N stretching vibration, but further evidence is needed for a reliable assignment. In view of its position and intensity, the IR band at 1006 cm^{-1} at pH 14 can be used as a marker for the ionic state His^{2-}.

The Raman spectra show a peak of medium intensity at 995 cm^{-1} from pH 0 to 13 and a second band that arises as a shoulder at 1007 cm^{-1} at pH 8 (Fig. 3). The bands have been proposed as tautomers markers for the N^{τ}- and N^{π}-protonated forms, respectively, of H_2His^0 and $HHis^-$ [16,21,22]. However, since the 995 cm^{-1} peak is also present at very low pH, this correlation can only be valid for the 1007 cm^{-1} component. Both bands have been assigned to =C–H in-plane bending vibrations [21,22,37] and ring deformations [24], but it has been demonstrated recently that the 995 cm^{-1} band is most likely a =C–N stretching coupled to a ring deformation [16]. The simultaneous presence of a weak IR band at the same position throughout the pH range is in line with this assignment and not in contradiction to the less detailed description of a =C–N stretching vibration [25] or a ring-stretching mode [23].

The IR and Raman bands below 990 cm^{-1} are mostly weak and assignments are only indicative. The weak shoulder in Raman around 970 cm^{-1} at acidic to neutral conditions have not been assigned in literature, but based on the observations and calculations for 4-methyl-imidazole, a coupled =C–N stretching and ring deformation is a plausible explanation for this band [14–17,37]. The large width of the IR band at 960 cm^{-1}, particularly at low pH, points to a vibration that is sensitive to hydrogen bonding. As the band disappears at pH >9, a deformation vibration of the NH_3^+ group is most likely causing this band. The usefulness of the band to mark conversion from $HHis^-$ to His^{2-} is limited regarding its low intensity. The weak Raman and IR band around 940 cm^{-1} that appears at pH ≥6 is assigned to an in-plane ring deformation in accordance with the literature on histidine [27,29] and 4-imidazole [12,15–18], but clearly different from the assignment to $\nu C–COO^-$ for histamine [47].

The Raman band at 920 cm^{-1} has been assigned to a =C–H deformation vibration [30], but this study concerned histidine in the crystalline state. Suggestions for the origin of the peak in spectra of aqueous solutions have not been found. The results for imidazole also point to a ring deformation vibration [12] and regarding the weak intensity of the band in both IR and Raman this assignment seems plausible. Occasionally, very weak Raman bands also appeared to be present in the region 910–890 cm^{-1}, but the origin of these peaks is not clear.

The weak to medium Raman band between 865 and 855 cm^{-1} has been assigned to a coupled =C–C stretching/ring deformation vibration [24], which is not fundamentally different from the suggestions that have been given for the IR band at this position [23,27,28]. Marti et al. [23] proposed a coupling of ν=C–C with νC–C–N for the IR band, which seems reasonable since the vibrations shows a higher Raman activity. However, the IR band is extremely broad and largely decreases in intensity on conversion from H_2His^0 to $HHis^-$ (pK_a = 9.1). This points to a contribution of an NH_3^+ deformation mode, possibly a rocking vibration as reported by Torreggiani et al. [37] for the histidine-related compound carnosine. For that reason, we propose a combination of both vibrations for the IR band.

The Raman spectra show two weak bands at 808 and 824 cm^{-1} up till pH 4 which turns into a single band at 820 cm^{-1} on increasing pH. The band has been attributed to a ring breathing vibration [24] and to a CO_2^- deformation vibration [30], but we prefer the assignment to =C–H out-of-plane deformation vibrations [28] as this is largely in line with the results of the theoretical studies on imidazole-related compounds [14,15,17,18,50].

The Raman shift at 782 cm^{-1} is only present up till pH 2 and therefore, it is a small but significant marker for the conversion of H_4His^{2+} to H_3His^+. Consequently, it is reasonable to assume that the band originates from a deformation vibration of the protonated carboxyl group, even though different assignments have been given to this vibrational frequency in the literature [24,36]. Unfortunately, IR data could not be obtained to confirm our proposal because of the opaqueness of the ATR crystal below 800 cm^{-1}. At first glance, it also seems difficult to extract an unambiguous assignment for the weak Raman band that is

observed in the pH range 0–8 between 699 and 718 cm^{-1}. Theoretical calculations on imidazole model compounds more or less agree on a combination of coupled ring =C–H bending modes [15,17,18], although some papers report on the involvement of a ring puckering and a N–H wagging mode [13,36]. The large contribution of ring =C–H deformation vibrations, however, is not in contrast to the assignment of a ring deformation mode that has been proposed for the Raman spectra of histidine [21,24,34] and therefore we assign the 718–699 cm^{-1} band accordingly. Similar arguments can be put forward for the Raman band that appears at 662 cm^{-1} when the pH is raised to 6 or higher, and the peak between 633 and 621 cm^{-1} that is present from pH 0 up to 13. The results of theoretical calculations point to coupled skeletal modes such as β=C–H and ν=C–C, which can be summarized as ring deformation vibrations [14–17,50]. This agrees well the assignments that are based on empirical data of histidine [21,23] and hence we assign both bands to skeletal ring deformation modes. Finally, assignment of the Raman band at 522 cm^{-1} to a COO– deformation vibration, as proposed in the literature [24,30], is doubtful as a band at this position is also present at pH 0. As we do not have a plausible alternative, we leave this band unassigned.

4. Conclusions

The combined measurement of the IR and Raman spectra of aqueous solutions of L-histidine over the pH range 0–14 provides a complete set of vibrational data that can be used to determine and monitor pH-induced structural changes. As such, the obtained information can be a useful contribution in the development of organic functionalized inorganic substrates with histidine as well as other amino acid compounds. The data collection allows a thorough integrated interpretation of the complementary spectral data, which leads to a higher reliability of the peak assignments. As a result, we have been able to confirm, correct and add conclusions from previously published vibrational studies on histidine. Furthermore, we have demonstrated that the obtained set of vibrational data can be used to determine all possible states of protonation, i.e. H_4His^{2+}, H_3His^{+}, H_2His^{0}, $HHis^{-}$and His^{2-}. Besides, IR and Raman bands that represent the imidazole N^{π}- or N^{τ}-protonated tautomeric forms of H_2His^{0} and $HHis^{-}$ have been established. These bands as well as the ones that can be used to mark the conversion from one state of protonation to another are summarized in Table 3. The majority of the bands agree well with the empirical and theoretical correlations that have been proposed in literature, but in some cases modifications appeared to be necessary.

4.1. $H_4His^{2+} \rightarrow H_3His^{+}$

The fully protonated state H_4His^{2+} is easily determined from the strong IR and weak Raman active C=O stretching band at 1736 cm^{-1} and the corresponding C–O(H) stretching IR band at 1257 cm^{-1}. Furthermore, the IR band at 1537 cm^{-1} and a weak but characteristic Raman peak at 782 cm^{-1} can be used to determine the presence of H_4His^{2+}. Other Raman shifts at 1632, 1494 and 1196 cm^{-1} are also prominent but these remain present in the spectra of H_3His^{+}. In agreement with the pK_a value of the carboxyl group, the disappearance of the corresponding C=O and C–O(H) bands around pH 2 mark the conversion to the H_3His^{+}. Concomitantly, the IR active anti-symmetric and symmetric C–O stretching of the CO_2^{-} group arise, the first one as a shoulder around 1600 cm^{-1} on the 1623 cm^{-1} band and the second one as a band of medium intensity at 1403 cm^{-1}. Finally, the IR band at 1537 cm^{-1} shifts to 1520 cm^{-1} and in Raman weak bands show up at 1414 and 1324 cm^{-1}.

4.2. $H_3His^{+} \rightarrow H_2His^{0}$

Conversion from H_3His^{+} to the zwitterionic form H_2His^{0} by partial deprotonation of the imidazole ring (pH >6) is marked in the Raman spectra by the disappearance of the bands at 1631 and 1196 cm^{-1} and a large decrease in intensity of the peak at 1494 cm^{-1}. Simultaneously, a new Raman band appears around 1575 cm^{-1}, which indicates that the N^{τ}-protonated form is the dominant tautomer for H_2His^{0}. The same can be concluded from the Raman band at

Table 3
Characteristic IR and Raman bands for the different ionic states and tautomer forms of L-histidine

	H_4His^{2+}	H_3His^{+}	H_2His^{0} (N^{π}–H)	H_2His^{0} (N^{τ}–H)	$HHis^{-}$ (N^{π}–H)	$HHis^{-}$ (N^{τ}–H)	$HHis^{2-}$
IR	1736	1623	1600	1600	1560	1560	1567
	1621	1600(s)	1520	1520	1496	1496	1450
	1537	1520	1408	1408	1410	1410	1416
	1257	1403	1265	1286	1265	1286	
			1105	1088	1105	1087	1006
Raman	1735	1631	1575	1575	1588	1571	1525
	1632	1494	1494	1494	1488	1488	1253
	1494	1414	1357	1324	1357	1325	
	1196	1324	1286	1286	1265	1286	
	782	1196			1005	990	

The addition (s) means the band is a shoulder.

1286 cm^{-1}. The strong Raman bands at 1357 and 1324 cm^{-1} can be used as tautomer markers too, but only when taking into account the intensity and in combination with the 1575 and 1286 cm^{-1} bands, since other ionic forms also have peaks at these positions. In IR, the shifted band maximum from 1623 to 1600 cm^{-1} and the increased intensity of the 1407 cm^{-1} peak can be responded as good markers for the conversion to H_2His^0. In addition, the presence of the N^{τ}-protonated tautomer can be derived from the weak bands at 1265 and 1105 cm^{-1}, while the bands at 1286 and 1088 cm^{-1} represent the N^{π}-protonated form.

4.3. $H_2His^0 \rightarrow HHis^-$

On further increasing the pH to higher than 9, the conversion to $HHis^-$ is reflected in a downward shift of the IR band at 1600–1560 cm^{-1}. Besides, a weak but characteristic band appears at 1496 cm^{-1}, while the 1410 cm^{-1} peak decreases in intensity. The position of the IR bands at 1265 and 1105 cm^{-1} and the ones at 1286 and 1088 cm^{-1} that reflect the N^{τ} and N^{π} tautomers, respectively, remain virtually unaffected. In Raman, two bands grow in at 1588 and 1265 cm^{-1} more or less proportional to the conversion to $HHis^-$. The increasing intensity of the shoulder at 1005 cm^{-1} on the band at 990 cm^{-1} is due to the same effect; i.e. an increasing amount of the N^{π}-protonated form for $HHis^-$. The 1488, 1357 and 1325 cm^{-1} bands remain constant.

4.4. $HHis^- \rightarrow His^{2-}$

The conversion from $HHis^-$ to His^{2-} is marked by a considerable change in the Raman spectra as all bands related to the N^{τ}- and N^{π}-protonated tautomers disappear. Firstly, the highly Raman active C=C stretching band around 1580 cm^{-1} shifts upon deprotonation of the imidazole ring to 1525 cm^{-1}. Secondly, the prominent bands at 1488, 1286 and 1160 cm^{-1} disappear, whereas a strong peak at 1253 cm^{-1} arises. Finally, the IR band at 1560 cm^{-1} shifts slightly upwards to 1567 cm^{-1} and the weak band around 1496 cm^{-1} disappears whereas new IR peaks at 1450 and 1006 cm^{-1} further illustrate the conversion to His^{2-}.

Acknowledgments

The authors thank the financial support from a Van der Leeuw/NWO-CW grant, a NRSCC grant and a NWO-CW-VICI grant.

References

[1] L. Stryer, Biochemistry, W.H. Freeman and Company, New York, 1988.
[2] E. Goormaghtigh, V. Cabiaux, J.-M. Ruysschaert, Subcell. Biochem. 23 (1994) 329.
[3] E. Li-Chan, S. Nakai, M. Hirotsuka, Protein Struct. Funct. Relat. Foods (1994) 163.
[4] A. Barth, Prog. Biophys. Mol. Biol. 74 (2000) 141.
[5] C. Jung, J. Mol. Recognit. 13 (2000) 325.
[6] A. Barth, Prog. Biophys. Mol. Biol. 74 (2001) 141.
[7] A. Barth, C. Zscherp, Q. Rev. Biophys. 35 (2002) 369.
[8] A.T. Tu, J. Chin. Chem. Soc. 50 (2003) 1.
[9] F.R. Dollish, W.G. Fateley, F.R. Bentley, Characteristic Raman frequencies of Organic Compounds, Wiley, New York, 1974.
[10] D. Lin-Vien, N.B. Colthup, W.G. Fateley, J.G. Graselli, The Handbook of Characteristic Infrared and Raman Frequencies of Organic Molecules, Academic Press, London, 1991.
[11] P. Hudaky, A. Perczel, J. Phys. Chem. A 108 (2004) 6195.
[12] S. Hashimoto, K. Ono, H. Takeuchi, I. Harada, Spectrochim. Acta A 50 (1994) 1647.
[13] J. Sadlej, A. Jworski, K. Miaskiewicz, J. Mol. Struct. 274 (1992) 247.
[14] M. Majoube, P. Millie, G. Vergoten, J. Mol. Struct. 344 (1995) 21.
[15] K. Hasegawa, T. Ono, T. Noguchi, J. Phys. Chem. B 104 (2000) 4253.
[16] A. Toyoma, K. Ono, S. Hashimoto, H. Takeuchi, J. Phys. Chem. A 106 (2002) 3403.
[17] K. Hasegawa, T. Ono, T. Noguchi, J. Phys. Chem. A 106 (2002) 3377.
[18] H. Gallouj, P. Lagant, G. Vergoten, J. Raman Spectrosc. 28 (1997) 909.
[19] D. Garfinkel, J.T. Edsall, J. Am. Chem. Soc. 80 (1958) 3807.
[20] F.P. Robinson, S.N. Vinogradov, Appl. Spectrosc. 18 (1964) 234.
[21] I. Ashikawa, K. Itoh, Biopolymers 18 (1979) 1859.
[22] I. Ashikawa, K. Itoh, Chem. Lett. 7 (1978) 681.
[23] E.M. Marti, Ch. Methivier, P. Dubot, C.M. Pradier, J. Phys. Chem. B 107 (2003) 10785.
[24] S. Martusevičius, G. Niaura, Z. Talaikyte, V. Razumas, Vib. Spectrosc. 10 (1996) 271.
[25] T. Noguchi, Y. Inoue, X.-S. Tang, Biochemistry 38 (1999) 10187.
[26] N. Wellner, G. Zundel, J. Mol. Struct. 317 (1994) 249.
[27] R.H. Carlson, T.L. Brown, Inorg. Chem. 5 (1966) 57.
[28] S.R. de Andrada Leite, M.A. Coutos dos Santos, C.R. Carobelli, A.M. Galindo Massabni, Spectrochim. Acta A 55 (1999) 1185.
[29] D.S. Caswell, T.G. Spiro, J. Am. Chem. Soc. 108 (1986) 6470.
[30] J.L.B. Faria, F.M. Almeida, O. Pilla, F. Rossi, J.M. Sasaki, F.E.A. Melo, J. Mendes Filho, P.T.C. Freire, J. Raman Spectrosc. 35 (2004) 242.
[31] T. Miura, T. Satoh, A. Hori-i, H. Takeuchi, J. Raman Spectrosc. 29 (1998) 41.
[32] T. Miura, A. Hori-i, H. Mototani, H. Takeuchi, Biochemistry 38 (1999) 11560.
[33] X. Zhao, D. Wang, T.G. Spiro, Inorg. Chem. 37 (1998) 5414.
[34] S. Stewart, P.M. Fredericks, Spectrochim. Acta A 55 (1999) 1641.
[35] M. Tasumi, I. Harada, T. Takamatsu, S. Takahashi, J. Raman Spectrosc. 12 (1982) 149.
[36] L.M. Markham, L.C. Mayne, B.S. Hudson, M.Z. Zgierski, J. Phys. Chem. 97 (1993) 10319.
[37] A. Torreggiani, M. Tamba, G. Fini, Biopolymers 57 (2000) 149.
[38] A.-M. Bellocq, C. Garrigou-Lagrange, J. Chim. Phys. Phys. Chim. Biol. 66 (1969) 1511.
[39] I.N. Jakab, K. Hernadi, D. Méhn, T. Kollár, I. Pálinkó, J. Mol. Struct. 651–653 (2003) 109.
[40] J.A. Cuadrado, W. Zhang, W. Hang, V. Majidi, J. Environ. Monit. 2 (2000) 355.
[41] S. Hashimoto, K. Ono, H. Takeuchi, J. Raman Spectrosc. 29 (1998) 969.
[42] J.G. Mesu, D. Baute, H.J. Tromp, E.E. van Faassen, B.M. Weckhuysen, Stud. Surf. Sci. Catal. 143 (2002) 287.
[43] D. Baute, D. Arieli, F. Neese, H. Zimmermann, B.M. Weckhuysen, D. Goldfarb, J. Am. Chem. Soc. 126 (2004) 11733.

[44] G. Tzvetkov, G. Koller, Y. Zubavichus, O. Fuchs, M.B. Casu, C. Heske, E. Umbach, M. Grunze, M.G. Ramsey, F.P. Netzer, Langmuir 20 (2004) 10551.
[45] W.F. Reynolds, I.R. Peat, M.H. Freedman, J.R. Lyerla, J. Am. Chem. Soc. 95 (1973) 328.
[46] F. Blomberg, W. Maurer, H. Ruterjans, J. Am. Chem. Soc. 99 (1977) 8149.
[47] K. Furić, V. Mohaček, M. Bonifačić, I. Štefanić, J. Mol. Struct. 267 (1992) 39.
[48] J.-J. Max, M. Trudel, C. Chapados, Appl. Spectrosc. 52 (1998) 226.
[49] J.A. Collado, I. Tuñon, E. Silla, F.J. Ramirez, J. Phys. Chem. A 104 (2000) 2120.
[50] F.J. Ramirez, I. Tuñon, J.A. Collado, E. Silla, J. Am. Chem. Soc. 125 (2003) 2328.
[51] S. Olsztynska, K. Komorowska, L. Vrielynck, N. Dupuy, Appl. Spectrosc. 55 (2001) 901.